Bioelectrocatalytic Conversion from N_2 to Chiral Amino Acids in a H_2/α-keto Acid Enzymatic Fuel Cell

Hui Chen, † Matthew B. Prater,† Rong Cai, †‡ Fangyuan Dong,† Hsiaonung Chen, † and Shelley D. Minteer*,†

† Department of Chemistry, University of Utah, 315 South 1400 East, RM 2020, Salt Lake City, Utah 84010, United States

* Corresponding Author: Shelley D. Minteer (minteer@chem.utah.edu)

KEYWORDS: N_2 conversion, enzymatic electrosynthesis, enzymatic fuel cell, chiral amino acid, self-powered

ABSTRACT: Enzymatic electrosynthesis is a promising approach to produce useful chemicals with the requirement of external electrical energy input. Enzymatic fuel cells (EFCs) are devices to convert chemical energy to electrical energy via the oxidation of fuel at the anode and usually the reduction of oxygen or peroxide at the cathode. The integration of enzymatic electrosynthesis with EFC architectures can simultaneously result in the self-powered enzymatic electrosynthesis with more valuable usage of electrons to produce high value-added chemicals. In this study, a H_2/α-keto acid EFC was developed for the conversion from chemically inert nitrogen gas to chiral amino acids powered by H_2 oxidation. A highly efficient cathodic reaction cascade was first designed and constructed. Powered by an applied voltage, the cathode supplied enough reducing equivalents to support the NH_3 production and NADH recycling catalyzed by nitrogenase and diaphorase. The produced NH_3 and NADH were in situ reacted with leucine dehydrogenase (LeuDH) to generate *L*-norleucine with 2-ketohexanoic acid as the NH_3 acceptor. 92% NH_3 conversion ratio and 87.1% Faradaic efficiency were achieved. On this basis, a H_2 powered fuel cell with hyper thermostable hydrogenase (SHI) as the anodic catalyst was combined with the cathodic reaction cascade to form the H_2/α-keto acid EFC. After 10 hours of reaction, the concentration of *L*-norleucine achieved 0.36 mM with > 99% enantiomeric excess (ee_p) and 82% Faradaic efficiency. From the broad substrate scope and the high enzymatic enantioselectivity of LeuDH, the H_2/α-keto acid EFC is an energy-efficient alternative to electrochemically produce chiral amino acids for biotechnology applications.

INTRODUCTION

Enzymatic electrosynthesis (EES) is an interdisciplinary research area that combines enzymatic catalysis with electrochemical techniques for the production of value-added chemicals.[1] EES has been studied recently, because it combines the advantages of high activity and selectivity of enzymatic catalysis and the utilization of clean and renewable electricity as the power source of electrochemical techniques. However, most enzymatic electrosynthesis systems require an external electrical energy input.[2] Enzymatic fuel cells (EFCs) are devices that incorporated enzymes as electrocatalysts at either the anode and/or cathode of a fuel cell, which is further used to convert the chemical energy from a fuel (such as glucose, formic acid, ethanol, and hydrogen) into electrical energy in the presence of oxygen or peroxide, under mild conditions (near neutral pH and temperatures from room temperature to 45°C).[2-4] The generated electrons at the anode flow through the external electric circuit to the cathode and are simply used to reduce the oxidants, oxygen or peroxides in most cases, to water.[5-6] The reactions in the cathodic compartment are only needed to ensure the generation of current. In recent years, enzymatic electrosynthetic reactions have been integrated into the EFC architecture to form a self-powered bioelectrocatalytic system. In this system, the enzymatic electrosynthetic reactions in the cathode compartment consume the electrons generated at the anode to enable the synthesis of valuable chemicals instead of low value-added water.[6-7] This integration simultaneously realizes the self-powered enzymatic electrosynthesis without external electrical energy input and the more valuable usage of electrons to produce chemicals with high added-value. For instance, Minteer's group reported the bioelectrocatalytic reduction of N_2 to NH_3 at the biocathode of a hydrogen EFC,[8] as well as a H_2/heptanal EFC to produce alkanes from aldehydes and alcohols.[9] EFCs have also been combined with enzymatic electrosynthesis cell to realize the production of l-3,4-dihydroxyphenylalanine powered by glucose oxidation.[2] Besides the issue of electron utilization, another problem which limits the application of EFCs is the poor operational stability due to the deactivation of enzymes resulting in short lifetimes and higher costs.[6] The enzyme stability in EFCs can be significantly improved by using enzyme immobilization via physical adsorption, entrapment, covalent binding or cross-linking. Once immobilized, enzymes usually obtained extended lifetime compared to the

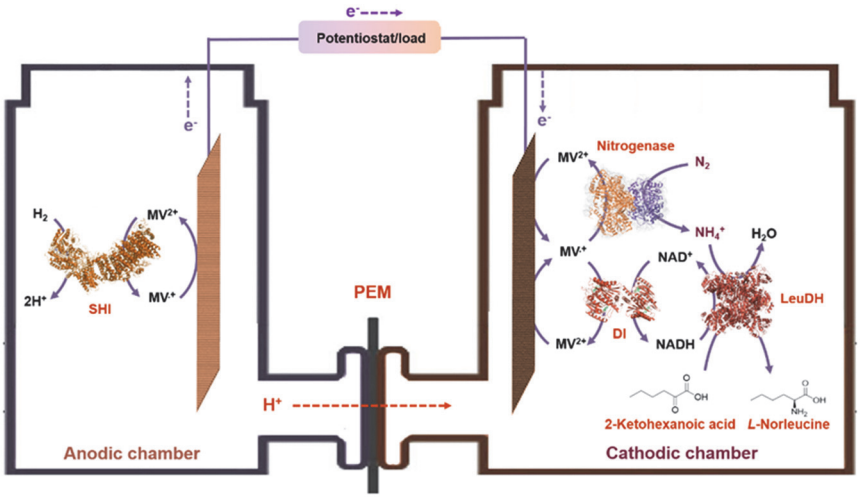

Figure 1. The schematic representation of the H_2/α-keto acid EFC

free enzymes.[10] The use of thermoenzymes or protein engineering enzymes for better stability is another easy way to improve the operation stability of EFCs.[6, 11-13] The thermoenzymes with high structural stability are able to stay stable and remain active for a long time and finally can be used to improve the operational stability of EFCs. Compared with immobilization, the use of thermoenzyme has greater application potential as it does not require the modification process of the electrode and avoids the loss of enzyme activity. The scale of EFCs is also a factor affecting their practical applications. Scale up of EFCs is expected to obtain higher power density output and more target products. However, there are considerable challenges to develop EFCs to be a large scale power source including the cost of enzyme preparation, the modification of electrode and the construction of reaction system.[14]

Dinitrogen (N_2) is the most abundant natural gas and also the ultimate source of nitrogen for nitrogenated industrial and natural compounds.[15] However, the fixation and conversion of N_2 to useful nitrogenous compounds is difficult due to the inertness of N_2.[16] So far, the fully hydrogenated product, ammonia (NH_3), is the most common product of N_2 fixation [16-17] This NH_3 product is produced industrially by the Haber-Bosch process which produces the NH_3 from hydrogen (H_2) and N_2 at the expense of 2% of global energy use and 3% of global CO_2 emission.[18-19] Minteer's group constructed a H_2/N_2 EFC capable of producing NH_3 from N_2 and H_2 at ambient conditions.[8, 20] In this H_2/N_2 EFC, the electrons generated at the hydrogenase anode were utilized at the nitrogenase cathode to perform the N_2 reduction and NH_3 production with 26.4 % Faradaic efficiency. A noteworthy issue herein is NH_3, the end-product of both the Haber-Bosch process and the H_2/N_2 EFC, is a commodity chemical. The conversion of NH_3 to nitrogenous chemicals with high added-value and complicated structure still requires further tedious chemical synthesis with the use of precious metal catalysts.[21] Therefore, it is necessary to develop a new system in which the generated NH_3 could be in situ converted by a cascade of reaction steps to a useful intermediate chemical that could be used as a building block for pharmaceutical or other biotechnological chemical production. In our recent research, we established an upgraded bioelectrocatalytic N_2 fixation system in which the chemically inert N_2 was captured and reduced by nitrogenase to produce NH_3, followed by transfer to alanine by *L*-alanine dehydrogenase and finally utilized by ω-transaminase to produce chiral amines at mild condition without precious metal catalysts.[22] Although the result has proved that it is feasible for the product of N_2 fixation to surpass NH_3, there were still three deficiencies which need to be further improved. 1. The low utilization ratio of generated NH_3 (approximately 40%); 2. The low faradaic efficiency (approximately 27.6%); and 3. The system relies on the external electrical energy input.

In order to realize the comprehensive conversion and application of N_2, the efficient in situ utilization of NH_3 generated from N_2 reduction is a critical step. Amino acid dehydrogenase (AADH, EC 1.4.1.9) is a group of enzymes which are able to utilize NH_3/NH_4^+ as a substrate to catalyze asymmetric reductive amination of α-keto acids to produce a variety of chiral amino acids with fast reaction rates, excellent enantioselectivity, and high atom economy.[23-27] This is interesting to the field, because chiral amino acids are used as precursors in the food, agricultural, and pharmaceutical industries, as well as used as chiral directing auxiliaries and chiral synthons in organic synthesis.[23, 26] Since the reactions catalyzed by AADH consume reduced equivalents, the efficient supply and regeneration of reduced cofactor is essential to ensure a smooth reaction.[28] The traditional enzymatic approach for coenzyme regeneration is to add a second enzymatic reaction which involves a second enzyme and a second substrate. Through the oxidation of the second substrate, the reduced cofactor can be regenerated. In comparison to enzyme-coupled cofactor regeneration, the bioelectrocatalytic approach for cofactor regeneration uses the electrode to electrochemical regenerate the cofactor. This method has long been acknowledged as potentially powerful, since it directly uses low-cost electricity as a regenerating reagent without the need of a second enzymatic system, the reaction process is

easy to monitor, and the potential can be controlled to ensure high Faradaic efficiency.[29-30] The bioelectrocatalytic cofactor regeneration has been widely used in the CO_2 fixation,[31-33] N_2 fixation,[8, 20] electrosynthesis of biofuels,[9, 34] and value-added chemicals,[2, 35-36] especially chiral chemicals.[22, 37-38]

In this study, we constructed an H_2/α-keto acid EFC to perform the conversion from chemically inert N_2 to chiral amino acids without an external electrical energy input. The electrons derived from the oxidation of H_2 were utilized to support the production of chiral amino acids instead of low value-added H_2O. The reaction cascade in the cathode chamber contained a nitrogenase (EC 1.18.6.1) from *Azotobacter vinelandii*, a diaphorase (DI, EC1.6.99.3) from *Geobacillus stearothermophilus*, and a *L*-leucine dehydrogenase (LeuDH, EC 1.4.1.9) from *Bacillus cereus* to perform the conversion from N_2 to a chiral amino acid. Methyl viologen (MV) was employed to mediate both the electron transfer between the carbon cathode and nitrogenase and the active site of diaphorase to realize the regeneration of NH_3 and NADH. The generated NH_3 and NADH were in situ utilized by LeuDH to perform the asymmetric amination of a variety of α-keto acid substrates and the generation of chiral amino acids. Finally, by employing a soluble [NiFe] hydrogenase I (SHI, EC1.12.1.3) from the hyperthermophilic archaeon, *Pyrococcus furiosus,* at the bioanode and a N_2 conversion cascade at the biocathode, we successfully constructed an H_2/α-keto acid EFC which was able to efficiently utilize the electrons generated from H_2 oxidation to realize the self-powered bioelectrocatalytic N_2 conversion with chiral amino acids as the final product.

RESULTS AND DISCUSSION

Design of the biocathode and EFC. As shown in **Figure 1**, a U-shaped dual-chamber electrochemical cell was used and separated by a Nafion proton exchange membrane (PEM). The protons generated from oxidation of H_2 catalyzed by SHI in the anodic chamber passed through Nafion into the cathodic chamber. The electrons moved from the anode to cathode and reduced the electron mediator, MV^{2+}, at the surface of the cathode. The reduced $MV^{\cdot+}$ was further utilized as reducing power for the reduction of N_2 catalyzed by nitrogenase and the regeneration of NADH catalyzed by DI. Due to the oxygen sensitivity of $MV^{\cdot-}$, SHI, and nitrogenase, a H_2/α-keto acid EFC requires anaerobic operation condition which can be easily constructed. In actual use, the ultra-high purity H_2 and N_2 need to be filled into the headspace of the anodic and cathodic chamber as they are the substrates of hydrogenase and nitrogenase, respectively. While filling ultra-high purity H_2 and N_2, anaerobic conditions can be obtained. Meanwhile, it is also possible for nitrogenase to catalyze N_2 reduction with air as the substrate. Previous research indicated that a "conformational switch" protein (FeSII or "Shethna") was able to protect nitrogenase upon exposure to O_2. Upon exposure to air in the presence of FeSII protein, 40% N_2 reduction activity can be preserved.[39] If the FeSII protein is supplemented into the cathodic chamber of the H_2/α-keto acid EFC, the nitrogenase would also be able to use air as the substrate and methyl viologen as the electron mediator to perform the N_2 reduction. For SHI in the anodic chamber, it can be immobilized via physical entrapment in the viologen-polymer redox hydrogel to prevent the hydrogenase from the O_2 damage as the electrons generated from H_2 oxidation catalyzed by hydrogenase can induce viologen catalyzed O_2 reduction at the surface of the polymer.[40] However, the target of this study is to obtain a high concentration of amino acids with high Faradaic efficiency. The addition of FeSII protein can only preserve 40% nitrogenase in the presence of O_2. Moreover, the existence of O_2 can also oxidize the reduced methyl viologen in both the anodic and cathodic chambers, which further significantly decrease the Faradaic efficiency. Based on the above considerations, the H_2/α-keto acid EFC was opeated under anaerobic conditions.

In order to address the problems of low NH_3 utilization ratio (approximately 40%) and low Faradaic efficiency (approximately 27.6%) of the previous upgraded N_2 fixation system,[22] the reaction and transfer pathway of NH_3 in the cathodic chamber was simplified to improve the transfer and capture efficiency. In detail, the reduced $MV^{\cdot+}$ generated at the cathode was employed as the electron donor for the N_2 reduction and NH_3 generation. Then, the generated NH_3 was captured and in situ utilized by LeuDH to produce *L*-norleucine and a variety of other chiral amino acids with different α-keto acids as the NH_3 acceptor. Meanwhile, the consumed NADH could be regenerated by DI and reduced $MV^{\cdot+}$. In comparison to the previous upgraded N_2 fixation system,[22] the further transformation process of generated amino acid, such as the reactions catalyzed by ω-transaminase with amino acids as amino group donor, was not integrated into the current system to simplify the transfer path of NH_3 and further improve the conversion efficiency from NH_3 to final products. On the basis of the highly efficient cathodic reaction cascade, the hydrogenase (SHI) anode was integrated into the system to form the H_2/α-keto acid EFC with H_2 as fuel. The electrons generated from H_2 oxidation were transported to the anode via reduced $MV^{\cdot+}$ and finally moved to the cathode to support the reactions occurring in the cathodic chamber.

It is important to note that the same mediator is being used in both the anodic and cathodic chambers for simplicity. This means there is no standard potential difference between the two chambers of the EFC, but the potential of the $MV^{2+}/MV^{\cdot+}$ redox couple at each electrode changes upon a shift in the equilibrium between MV^{2+} and $MV^{\cdot+}$ as per the Nernst equation owing to their respective enzymatic activities. The theoretical maximum open circuit voltage (OCV) for this system is 250 mV.[8]

Optimization of the nitrogenase concentration. As NH_3 is the substrate of LeuDH, a higher concentration of NH_3 is beneficial to the production and accumulation of chiral amino acids. In order to obtain high NH_3 concentrations, the concentration of nitrogenase was first optimized. As shown in **Figure 2**, the highest accumulation concentration of NH_3 depended on the concentration of nitrogenase. Increasing the nitrogenase concentration from 0.125

U/mL (0.2 mg/mL MoFe protein and 0.9 mg/mL Fe protein) to 0.250 U/mL (0.4 mg/mL MoFe protein and 1.8 mg/mL Fe protein) can make the final concentration of NH_3 increase from 1.3 mM to 2.1 mM. Further increase in nitrogenase concentration to 0.375 U/mL (0.6 mg/mL MoFe protein and 2.7 mg/mL Fe protein) led to the reduction of final NH_3 concentration (1.4 mM). Some previous studies also indicated that with the total protein concentration of nitrogenase increased (with the fixed MoFe protein/Fe protein molar ratio), the specific activity of nitrogenase decreased.[41-42] This inhibition is due to the mass-action effect on the equilibrium between $(MgADP)_2$ bound oxidized Fe protein and reduced MoFe protein. The dissociation of the complex (oxidized Fe protein)-$(MgADP)_2$-(reduced MoFe protein) is rate-limiting at high protein concentrations. The high total concentration of nitrogenase (0.6 mg/mL MoFe protein and 2.7 mg/mL Fe protein, 3.3 mg/mL total protein) is not conducive to the dissociation of oxidized Fe protein from the reduced MoFe protein and the re-association of the complex of reduced Fe protein and oxidized MoFe protein. Consequently, 0.25 U/mL nitrogenase (0.4 mg/mL MoFe protein coupled with Fe protein in a 1:16 mol/mol ratio) was the optimum concentration for NH_3 production.

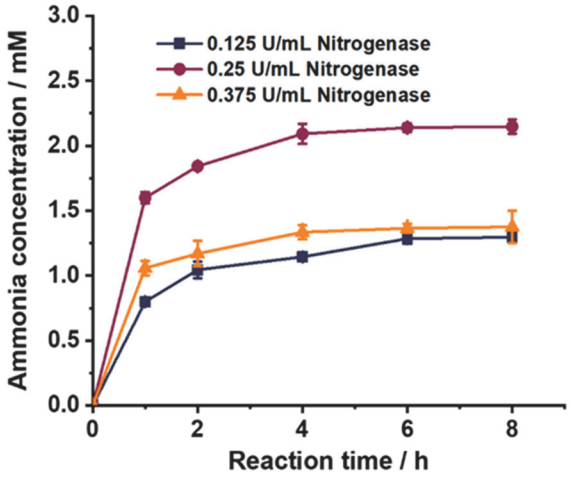

Figure 2. Optimization of nitrogenase concentration based on the concentration of generated NH_3. The data shown represent the means with standard deviations from triplicate experiments.

Potentiostatic electrolysis analysis of the reaction process. First, cyclic voltammetric (CV) analysis was used to show that MV^{2+} can act as the electron mediator between the cathode and both nitrogenase and DI (**Figure S2**). The CV of 100 μM $MV^{\cdot+}$ indicated that the oxidized MV^{2+} could be reduced to $MV^{\cdot+}$ at a potential of -0.75 V vs SCE. After the addition of 0.15 U/mL nitrogenase (MoFe/Fe protein ratio of 1:16), a current response was observed due to the turnover of nitrogenase at -0.75 V vs SCE. This current response demonstrated the electron transfer between the cathode and nitrogenase was mediated by MV^{2+}. After further adding 0.15 U/mL DI and 100 μM NAD^+, a larger current response was obtained at the same potential. This result demonstrated that the electrons mediated by MV^{2+}, utilized by DI and finally was transferred to NAD^+ to realize the recycling of NADH. To maintain a high current density for high conversion rates, the working electrode potential was set at -0.85 V vs. SCE for all other bulk electrolysis experiments.

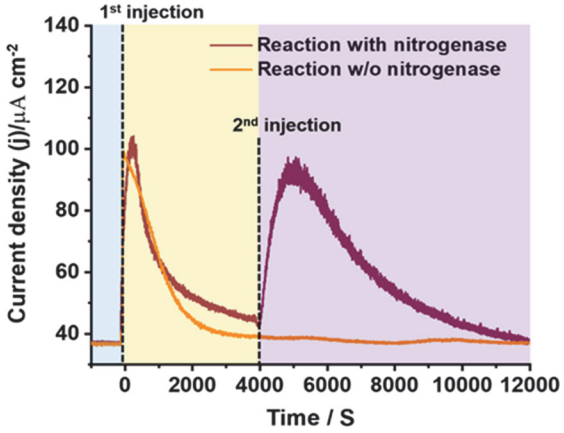

Figure 3. Amperometric *i*-t curve trace of the cathodic reaction. The MV^{2+} (1 mM) mediated N_2 reduction with and without nitrogenase was sequentially supplemented with components of NADH recycling (1st injection) and *L*-norleucine generation (2nd injection). In the 1st injection, 0.25 U/mL DI and 200 μM NAD^+ were added. In the 2nd injection, 2.5 mM 2-ketohexanoic acid (final concentration) and 0.45 U/mL LeuDH (final concentration) were added to the reaction mixture.

After determining the working electrode potential, the bulk electrolysis analysis was employed to trace the reaction process and further analyze the feasibility of the system design in this research (**Figure 3**). In the current versus time curve, there are three processes of interest that are separated by two injections. The first portion of the curve is the N_2 reduction and NH_3 generation catalyzed by nitrogenase with 1 mM MV^{2+} as the electron mediator. For the reaction without nitrogenase, only the MV^{2+} was reduced, since no NH_3 could be generated. After 5 hours of reaction, the system achieved steady-state and the current stabilized. Upon the addition of 0.25 U/mL DI and 200 μM NAD^+ to the electrolyte (1st injection), both the reaction with and without nitrogenase exhibited a dramatic increase in the reductive current. This current response reflects the reduction of NAD^+ catalyzed by DI with the reduced $MV^{\cdot+}$ as the electron donor. Upon the addition of 2.5 mM 2-ketohexanoic acid (final concentration) and 0.45 U/mL LeuDH (apparent activity, final concentration) (2nd injection), only the reaction with nitrogenase exhibited a statistically significant current response. This current response was probably the reflection of the formation of the final product, *L*-norleucine. The enzymatic consumption of NH_3, reduced $MV^{\cdot+}$ and regenerated NADH further accelerated the electron transfer from cathode to electrolyte and resulted in an enhanced current response. For the reaction without nitrogenase, no *L*-norleucine could be generated as there was no NH_3 in the electrolyte. Therefore, the current response could not be observed. The generation of *L*-norleucine in the reaction with nitrogenase was

confirmed by UPLC-MS and GC-MS (**Figure S3** and **Figure S4**).

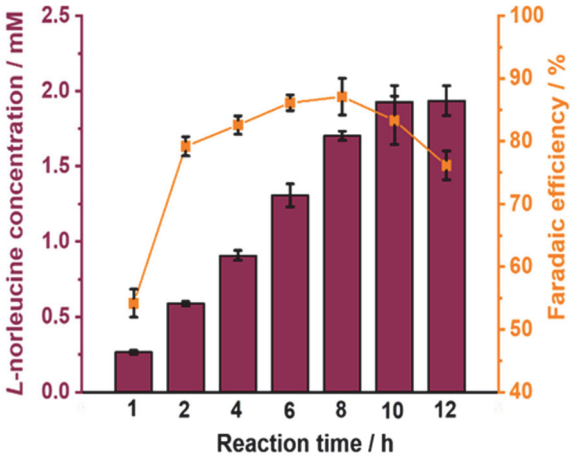

Figure 4. The concentration of *L*-norleucine generated in the bioelectrocatalytic N_2 conversion system powered by an applied voltage (-0.85 V vs SCE) and corresponding faradaic efficiency during the 12 hours time course. The concentrations represent the means from three separate individual U-shaped dual-chamber electrochemical cells. For every single cell, the concentrations were obtained based on triplicate amino acid derivatization.

Bioelectrocatalytic *L*-norleucine production powered by an applied voltage. In order to evaluate the efficiency of the reaction cascade in the cathodic chamber, the bioelectrocatalytic *L*-norleucine production powered by a potentiostat at -0.85 V vs SCE with 2.5 mM 2-ketohexanoic acid as substrate was performed. As shown in **Figure 4**, the concentration of generated *L*-norleucine achieved the highest level, 1.93 mM, after 10 hours of reaction. At this product concentration, the utilization ratio of NH_3 was up to 92% (the highest accumulation concentration is 2.1 mM, see **Figure 2**), which is approximately 2.3 times higher than that in our previous research (~ 40% NH_3 utilization ratio).[22] The highest Faradaic efficiency (87.1%) was observed with the 8 hour run. In comparison with our previous research (27.6% Faradaic efficiency),[22] the faradaic efficiency was increased approximately 3.4 times. Moreover, the Faradic efficiency of this study could be stably maintained above 75% from the 2nd hour to the 12th hour. The above results indicated that the generated NH_3 and electrons were more efficiently utilized and the performance of the cathodic reaction cascade was significantly improved in comparison with the previous research. In the previous research,[22] the generated NH_3 was transferred to pyruvate by *L*-alanine dehydrogenase to produce *L*-alanine. Then, the generated L-alanine utilized by ω-transaminase as an amino group donor to produce a chiral amine and pyruvate. For the reaction catalyzed by ω-transaminase, the equilibrium is on the side of the substrate (ketone and alanine) but not on the side of the products (amine and pyruvate).[43] The co-product, pyruvate, cannot be accumulated and needs to be promptly converted to alanine with the consumption of generated NH_3 to push the reaction equilibrium to the side of amine product. A low concentration of pyruvate is conducive to the generation of the amine. In the previous research, the concentration of pyruvate was only 50 μM, which was well below the K_m value of L-alanine dehydrogenase towards pyruvate (880 μM).[44] In this study, the reaction catalyzed by ω-transaminase has not been integrated into the reaction system to simplify the transfer path of NH_3. More importantly, the concentration of NH_3 acceptor, 2-ketohexanoic acid, was 2.5 mM, which was higher than the K_m value of LeuDH towards 2-ketohexanoic acid (1.2 mM).[45] The generated NH_3 was more efficiently captured and utilized. Finally, the concentration of product (1.93 mM) was approximately 3.4 times higher than that of previous research (0.56 mM).

EFC performance. The soluble [NiFe] hydrogenase I (SHI, EC1.12.1.3) from the hyperthermophilic archaeon, *Pyrococcus furiosus,* is a hyper thermostable hydrogenase which can stay stable and continuously work at 70°C, or even 80°C, for dozens of hours.[46-47] In addition to hydrogen production, the reversible nature of the SHI reaction also allows it to perform the oxidation of hydrogen and the reduction of the electron mediator.[48] These properties make SHI is a good candidate to construct a H_2 fuel cell. Since it was the first time for SHI to be used in an EFC, it is necessary to determine its electrochemical properties and evaluate the performance of the newly constructed EFC. From the CV in **Figure 5a**, the decreased reductive current response at -0.73 V vs SCE and the increased oxidative current response at -0.65 V vs SCE indicated the oxidative MV^{2+} was reduced to $MV^{\cdot+}$ by SHI via the oxidation of H_2. This result in comparison to the control with BSA and the blank without hydrogen provide evidence of mediated bioelectrocatalysis. **Figure 5b** further demonstrated the electrochemical oxidation of reduced $MV^{\cdot+}$ that is produced by SHI via H_2 oxidation by using potentiostatic bulk electrolysis analysis. After the bubbling of H_2, the oxidative MV^{2+} was reduced by SHI with H_2 as an electron donor. Then, the reduced $MV^{\cdot+}$ was oxidized at the working electrode to produce the oxidative current. **Figure 5C** shows the evolution of open-circuit voltage (OCV) for the H_2/α-keto acid EFC, where the anodic chamber contained 10 mM oxidized MV^{2+} and 100% H_2 0.1 mg/mL SHI was injected into anodic chamber at 300s The cathodic chamber contained 0.25 U/mL nitrogenase, 0.25 U/mL DI, 0.45 U/mL LeuDH (apparent activity), 1 mM reduced $MV^{\cdot+}$, 2.5 mM 2-ketohexanoic acid, and 100% N_2. $MgCl_2$ (6.7 mM) and NAD^+ (200 μM) were added into the cathodic chamber at 1500s to initiate nitrogenase and DI turnover, as it is required for biocatalytic function. After allowing the OCV to evolve for 2500s, the OCV stabilized at approximately 248 ± 6 mV which was close to the theoretical maximum potential.[8] After the determination of the OCV, the performance of the EFC was evaluated by slow linear polarization (0.5 mV/s) from OCV to short circuit (**Figure 5d**). The maximum current and power densities were 42 ± 3 μA/cm² and 1.45 ± 0.18 μW/cm². This result also proves that SHI can be used to construct EFC. When the EFC had a maximum power output (1.45 μW/cm²), the corresponding potential is 75 mV.

Consequently, the working potential of the EFC was held at 75 mV.

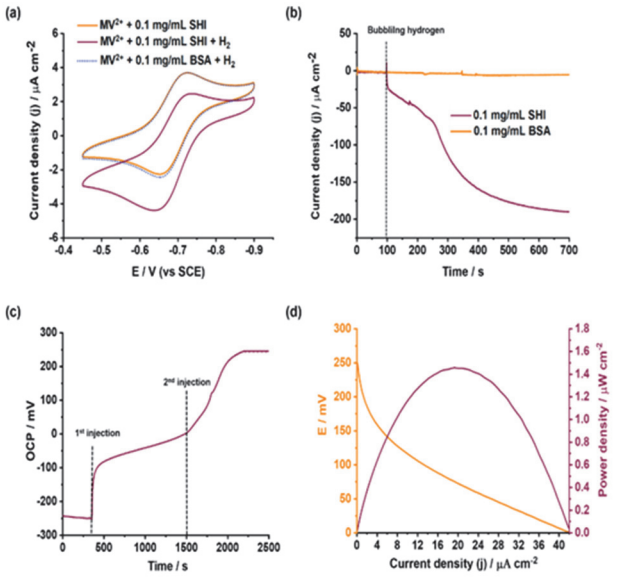

Figure 5. The performance of H_2/α-keto acid EFC. (a) Representative CVs of the oxidation of H_2 catalyzed by SHI with oxidized MV^{2+} as the electron acceptor. (b) Bulk electrolysis current versus time curve for the MV^{2+} mediated oxidation of H_2 by SHI. (c) Representative OCV stabilization of the H_2/α-keto acid EFC. 0.1 mg/mL SHI was added into the anodic chamber at 300 s (1st injection). 6.7 mM $MgCl_2$ and 200 μM NAD^+ were added into the cathodic chamber at 1500 s to initiate nitrogenase and DI turnover (2nd injection). (d) Representative polarization and power curves of the H_2/α-keto acid EFC.

Fuel cell-powered bioelectrosynthetic *L*-norleucine production. After getting the highly efficient cathodic reaction cascade, the H_2 fuel cell was integrated into the bioelectrocatalytic system to construct the H_2/α-keto acid EFC which was further used to perform the bioelectrocatalytic conversion from N_2 to *L*-norleucine. As shown in **Figure 6**, the *L*-norleucine concentration of the reaction powered by the EFC achieved the highest level, 0.36 mM, after 10 hours of reaction. Although the concentration of *L*-norleucine of the reaction powered by EFC was decreased compared with that of reaction powered by an applied voltage, the Faradaic efficiency still remained at a high level. The Faradaic efficiency of the reaction powered by the EFC was maintained at approximately 82% from the 2nd hour to the 6th hour. After 6th hour, the Faradaic efficiency exhibited a downward trend. When the reaction was over, the Faradaic efficiency was 64% which was still 2.5 times higher than the highest Faradaic efficiency (27.6%) of the previous research.[22] The above results indicate that the H_2/α-keto acid EFC is able to work without external electrical energy input. The electrons generated from the oxidation of H_2 were utilized by the cathodic reaction cascade for the conversion from chemically inert N_2 to *L*-norleucine with high Faradaic efficiency. As the same electron mediator is being used in both the anodic and cathodic chamber, the limited maximum OCV (250 mV, **Figure 5c**) limited the power density output of the H_2/α-keto acid EFC. As a result, the concentration of reduced $MV^{\cdot+}$ in the cathodic chamber was not high enough to fully support the N_2 reduction catalyzed by nitrogenase and the NADH regeneration catalyzed by DI. That was the reason why the final *L*-norleucine concentration of the reaction powered by the H_2/α-keto acid EFC was lower than that of reaction powered by the potentiostat. One the other hand, the MV^{2+} with low reductive potential (-0.75V vs SCE) was considered to be the best electron mediator of nitrogenase for the N_2 reduction.[49] It is difficult to find another electron mediator with lower reductive potential used in the anodic chamber to construct the H_2/α-keto acid EFC and generate high OCV. Although the use of the same mediator in both the anodic and cathodic chamber only generated 250 mV OCV, it still successfully drove the H_2/α-keto acid EFC and generate *L*-norleucine with high Faradaic efficiency. Future work could explore other mediator systems to increase produced potential for improved efficiency.

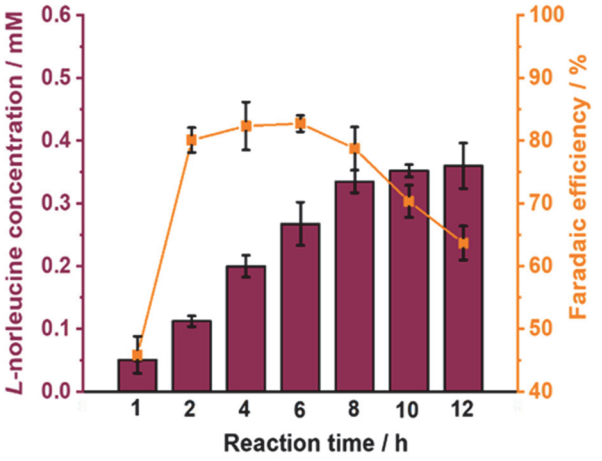

Figure 6. The concentration of *L*-norleucine generated in the H_2/α-keto acid EFC and corresponding faradaic efficiency at 12 hour time course. The concentrations represent the means from three separate individual U-shaped dual-chamber electrochemical cells. For every single cell, the concentrations were obtained based on triplicate amino acid derivatization.

Bioelectrosynthetic reductive amination of different α-keto acid substrates. LeuDH shows activity toward straight and branched chain α-keto acids as well as some alicyclic α-keto acids.[50] From the wide substrate scope of LeuDH, the H_2/α-keto acid EFC is able to produce a variety of chiral amino acids. Herein, 6 prochiral α-keto acids with different structures (**Figure 7**) were employed as a substrate in the H_2/α-keto acid EFC to produce corresponding chiral amino acids (**Figure S5**). After 10 hours of electrolysis, most α-keto acid substrates were converted to the corresponding amino acids (**Table 1**). The concentration of produced *L*-norleucine (1b, 0.36 mM), *L*-norvaline (2b, 0.38 mM), *L*-valine (3b, 0.4 mM), and *L*-tert-leucine (4b, 0.4 mM) were almost at the same level. The concentration of the generated *L*-cyclopropyl glycine (6b) was 0.28 mM, which was lower than the concentration of other products.

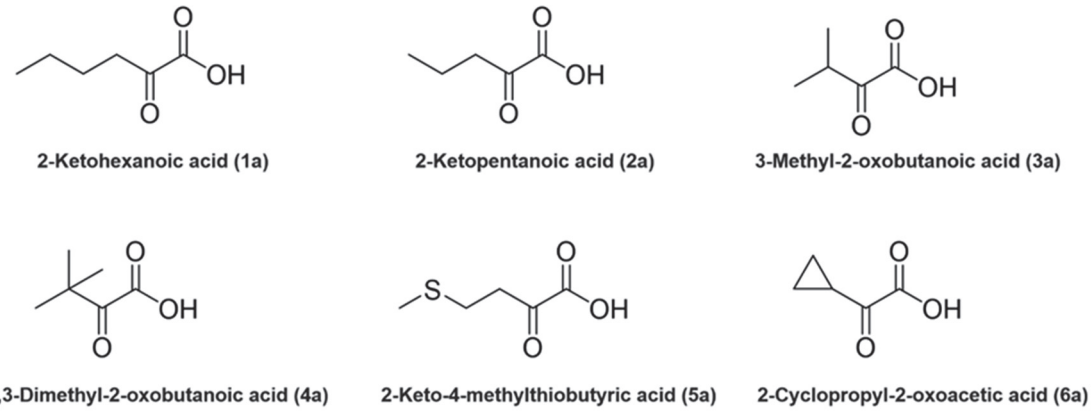

Figure 7. Prochiral α-keto acid as substrates of H_2/α-keto acid EFC used to produce chiral amino acids

Table 1. Asymmetric amination of various α-keto acid by the H_2/α-keto acid EFC[a]

substrate	product	product concentration (mM)	ee_p (%)[b]	yield rate (μmol·L^{-1}·h^{-1})
1a	**1b**	0.36 ± 0.036	>99 (L)	36
2a	**2b**	0.38 ± 0.014	>99 (L)	38
3a	**3b**	0.40 ± 0.016	95.2 (L)	40
4a	**4b**	0.40 ± 0.022	>99 (L)	40
5a	**5b**	n.d.[c]	n.d.[c]	n.d.[c]
6a	**6b**	0.28 ± 0.012	>99 (L)	28

[a] Values represent the means from three separate individual U-shaped dual-chamber electrochemical cells. For every single cell, the values were obtained based on triplicate amino acid derivatization.
[b] In [%]. Determined by SFC after derivatization.
[c] n.d. Not determined because of too low a conversion

The amination product of substrate 5a (2-keto-4-methylthiobutyric acid) was not determined due to too low concentration. Previous research indicated that the reduced amination activity of LeuDH from *Bacillus cereus* towards 2-keto-4-methylthiobutyric acid was much lower than that towards regular aliphatic α-keto acids.[51] As the crystal structure of LeuDH from *Bacillus cereus* has not been obtained, it can only be speculated that the larger atomic radius and stronger polarity of the sulfur atom compared with carbon atom cause the 2-keto-4-methylthiobutyric acid cannot be well-positioned in the active pocket of LeuDH and finally lead to the low activity of LeuDH towards 2-keto-4-methylthiobutyric acid. Additionally, all of the generated products had excellent optical purity (**Table1** and SFC result in supporting information). Except for the generated *L*-valine (3b, ee_p = 95.2%), the ee_p value of all other products were > 99%. The obtained chiral amino acids are important intermediates of various high value-added chemicals, especially pharmaceutical intermediates. The hydroxylated product of *L*-norleucine, *L*-6-hydroxy-norleucine, is a chiral intermediate for the production of omapatrilat, indospicines, siderophores, and peptide hormone analogs.[50, 52] *L*-norvaline is a vital intermediate in the chemical synthesis of an antihypertensive drug, Perindopril.[53] *L*-valine is an essential amino acid for vertebrates.[54] *L*-tert-leucine is a valuable precursor for a variety of active pharmaceuticals, such as hepatitis C antiviral NS1 protease inhibitors (telaprevir, bocepravir), NS3/4 protease inhibitors (asunaprevir, faldaprevir, and vedroprevir), and HIV protease inhibitor (atazanavir).[50] *L*-cyclopropylglycine is an intermediate for the synthesis of a corticotropin-releasing factor-1 receptor antagonist.[55]

It can be expected that the bioelectrocatalytic N_2 conversion system can act as a platform to produce a variety of chiral amino acids with the integration of different AADHs. So far, 26 different subclasses for AADHs are listed in the Enzyme Nomenclature database. More than 24,770 amino acid sequences of AADHs are stored in the Uniport database, and 521 structures of AADHs are available in the Protein Data Bank. A few AADHs, such as glutamate dehydrogenase, phenylalanine dehydrogenase, *meso*-diaminopimelate dehydrogenase and leucine dehydrogenase have good potential as industrial biocatalysts for the reductive amination process.[50] Building on these research advances in AADHs, the H_2/α-keto acid EFC has an attractive possibility for the production of chiral amino acid with wide product scope. Compared with the traditional biocatalytic chiral amino acids production, the chiral amino acids in a H_2/α-keto acid EFC is a proof of concept research as some amino acids have been successfully produced on an industrial scale by using traditional biocatalytic methods.[50] However, the H_2/α-keto acid EFC exhibited an attractive possibility that the chemically inert N_2 could directly be converted to high value-added chiral amino acids via one-pot multi-enzymatic bioelectrosynthesis. Compared with regular EFC, the electrons were more valuable used instead of simply being reduced to water. The electrons generated from H_2 oxidation were utilized to realize the reduction of

N_2 and reductive amination α-keto acids to realize the production of chiral amino acids without the external electrical energy input or the addition of sacrificial agents and extra dehydrogenase for the regeneration of reduced equivalent. This H_2/α-keto acid EFC has the potential to realize the green and distributed manufacturing of chiral amino acids.

CONCLUSION

In this research, we demonstrated the feasibility of using a H_2/α-keto acid EFC to perform the bioelectrocatalytic conversion from chemically inert N_2 to chiral amino acids with high Faradaic efficiency. The hyper thermostable hydrogenase, SHI, was shown for the first time to be applicable in the construction of a H_2 fuel cell. In this H_2/α-keto acid EFC, the electrons generated from oxidation of H_2 were utilized to support the N_2 conversion. Moreover, the product of N_2 conversion went beyond ammonia and reached chiral amino acids at mild conditions without the requirement of precious metal catalysts or an external electrical energy input. Based on the solid research foundation of AADHs, the H_2/α-keto acid EFC is able to act as a platform to prepare a variety of amino acids with the integration of different AADHs.

ASSOCIATED CONTENT

Supporting Information. The supporting information is available free of charge via the Internet at http://pubs.acs.org."

The DNA and amino acid sequences of the proteins, material and methods, the SDS-PAGE gel of enzymes used in this study, representative cyclic voltammograms of the nitrogenase bioelectrocatalysis mediated by MV^{2+}, the UPLC-MS characterization of generated *L*-norleucine, the GC-MS characterization of generated *L*-norleucine, and the SFC analysis of the enaniomeric excess analysis of the generated amino acids in this study (PDF).

AUTHOR INFORMATION

Corresponding Author

* Shelley D. Minteer: minteer@chem.utah.edu

Present Addresses

ǂ R.C.: Department of Chemistry, University of California, Berkeley, California 94720, USA

ORDID

Hui Chen: 0000-0002-8944-0090
Shelley D. Minteer: 0000-0002-5788-2249

Notes

The authors declare no competing financial interest.

ACKNOWLEDGMENT

We thank Prof. Chun You (Tianjin Institute of Industrial Biotechnology, Chinese Academy of Science, China) and Prof. Thomas J. Santangelo (Department of Biochemistry and Molecular Biology, Colorado State University, USA) for the supplying pTE5 plasmid and *Thermococcus kodakarensis* KOD1 strain for the preparation of hydrogenase SHI. This study was supported by the Army Research Office MURI grant (#W911NF1410263) and the National Science Foundation Center for Synthetic Organic Electrosynthesis for funding (CHE-1740656).

REFERENCES

(1) Wu, R.; Ma, C.; Zhu, Z. Enzymatic electrosynthesis as an emerging electrochemical synthesis platform. *Curr. Opin. Electrochem.* **2020,** *19*, 1-7.

(2) Wu, R.; Zhu, Z. Self-Powered Enzymatic Electrosynthesis of l-3, 4-Dihydroxyphenylalanine in a Hybrid Bioelectrochemical System. *ACS Sustain. Chem. Eng.* **2018,** *6*, 12593-12597.

(3) Milton, R. D.; Lim, K.; Hickey, D. P.; Minteer, S. D. Employing FAD-dependent glucose dehydrogenase within a glucose/oxygen enzymatic fuel cell operating in human serum. *Bioelectrochemistry* **2015,** *106*, 56-63.

(4) Rasmussen, M.; Abdellaoui, S.; Minteer, S. D. Enzymatic biofuel cells: 30 years of critical advancements. *Biosens. Bioelectron.* **2016,** *76*, 91-102.

(5) Mazurenko, e.; De Poulpiquet, A.; Lojou, E. Recent developments in high surface area bioelectrodes for enzymatic fuel cells. *Curr. Opin. Electrochem.* **2017,** *5*, 74-84.

(6) Xiao, X.; Xia, H.-q.; Wu, R.; Bai, L.; Yan, L.; Magner, E.; Cosnier, S.; Lojou, E.; Zhu, Z.; Liu, A. Tackling the challenges of enzymatic (bio) fuel cells. *Chem. Rev.* **2019,** *119*, 9509-9558.

(7) Mazurenko, I.; Etienne, M.; Kohring, G.-W.; Lapicque, F.; Walcarius, A. Enzymatic bioreactor for simultaneous electrosynthesis and energy production. *Electrochim. Acta* **2016,** *199*, 342-348.

(8) Milton, R. D.; Cai, R.; Abdellaoui, S.; Leech, D.; De Lacey, A. L.; Pita, M.; Minteer, S. D. Bioelectrochemical Haber-Bosch Process: An Ammonia-Producing H_2/N_2 Fuel Cell. *Angew. Chem. Int. Ed.* **2017,** *56*, 2680-2683.

(9) Abdellaoui, S.; Macazo, F. C.; Cai, R.; De Lacey, A. L.; Pita, M.; Minteer, S. D. Enzymatic Electrosynthesis of Alkanes by Bioelectrocatalytic Decarbonylation of Fatty Aldehydes. *Angew. Chem. Int. Ed.* **2018,** *57*, 2404-2408.

(10) Ahmad, R.; Sardar, M. Enzyme immobilization: an overview on nanoparticles as immobilization matrix. *Biochem. Anal. Biochem.* **2015,** *4*, 1.

(11) Zhu, Z.; Tam, T. K.; Sun, F.; You, C.; Zhang, Y.-H. P. A high-energy-density sugar biobattery based on a synthetic enzymatic pathway. *Nat. Commun.* **2014,** *5*, 3026.

(12) Zhu, Z.; Ma, C.; Zhang, Y.-H. P. Co-utilization of mixed sugars in an enzymatic fuel cell based on an in vitro enzymatic pathway. *Electrochim. Acta* **2018,** *263*, 184-191.

(13) Zhu, Z.; Wang, Y.; Minteer, S. D.; Zhang, Y.-H. P. Maltodextrin-powered enzymatic fuel cell through a non-natural enzymatic pathway. *J. Power Sources* **2011,** *196*, 7505-7509.

(14) Gamella, M.; Koushanpour, A.; Katz, E. Biofuel cells-activation of micro-and macro-electronic devices. *Bioelectrochemistry* **2018,** *119*, 33-42.

(15) Jia, H. P.; Quadrelli, E. A. Mechanistic aspects of dinitrogen cleavage and hydrogenation to produce ammonia in catalysis and organometallic chemistry: relevance of metal hydride bonds and dihydrogen. *Chem. Soc. Rev.* **2014,** *43*, 547-564.

(16) Cherkasov, N.; Ibhadon, A.; Fitzpatrick, P. A review of the existing and alternative methods for greener nitrogen fixation. *Chem. Eng. Process* **2015,** *90*, 24-33.

(17) Foster, S. L.; Bakovic, S. I. P.; Duda, R. D.; Maheshwari, S.; Milton, R. D.; Minteer, S. D.; Janik, M. J.; Renner, J. N.; Greenlee, L. F. Catalysts for nitrogen reduction to ammonia. *Nat. Catal.* **2018,** *1*, 490.

(18) Kandemir, T.; Schuster, M. E.; Senyshyn, A.; Behrens, M.; Schlögl, R. The Haber–Bosch process revisited: On the real structure and stability of "ammonia iron" under working conditions. *Angew. Chem.* **2013,** *52*, 12723-12726.

(19) Chen, J. G.; Crooks, R. M.; Seefeldt, L. C.; Bren, K. L.; Bullock, R. M.; Darensbourg, M. Y.; Holland, P. L.; Hoffman, B.; Janik, M. J.; Jones, A. K. Beyond fossil fuel–driven nitrogen transformations. *Science* **2018,** *360*, eaar6611.

(20) Milton, R. D.; Abdellaoui, S.; Khadka, N.; Dean, D. R.; Leech, D.; Seefeldt, L. C.; Minteer, S. D. Nitrogenase bioelectrocatalysis: heterogeneous ammonia and hydrogen production by MoFe protein. *Energy Environ. Sci.* **2016,** *9*, 2550-2554.

(21) Balaraman, E.; Srimani, D.; Diskin-Posner, Y.; Milstein, D. Direct synthesis of secondary amines from alcohols and ammonia catalyzed by a ruthenium pincer complex. *Catal. Lett.* **2015,** *145*, 139-144.

(22) Chen, H.; Cai, R.; Patel, J.; Dong, F.; Chen, H.; Minteer, S. D. Upgraded Bioelectrocatalytic N_2 Fixation: From N_2 to Chiral Amine Intermediates. *J. Am. Chem. Soc.* **2019,** *141*, 4963-4971.

(23) Yin, X.; Liu, Y.; Meng, L.; Zhou, H.; Wu, J.; Yang, L. Rational Molecular Engineering of Glutamate Dehydrogenases for Enhancing Asymmetric Reductive Amination of Bulky α-Keto Acids. *Adv. Synth. Catal.* **2019,** *361*, 803-812.

(24) Zhang, J.; Zhu, T.; Wu, X.; Chen, Y. Enhancement of biocatalytic efficiency by increasing substrate loading: enzymatic preparation of l-homophenylalanine. *Appl. Microbiol. Biotechnol.* **2013,** *97*, 8487-8494.

(25) Zhu, L.; Wu, Z.; Jin, J.-M.; Tang, S.-Y. Directed evolution of leucine dehydrogenase for improved efficiency of L-tert-leucine synthesis. *Appl. Microbiol. Biotechnol.* **2016,** *100*, 5805-5813.

(26) Vedha-Peters, K.; Gunawardana, M.; Rozzell, J. D.; Novick, S. J. Creation of a broad-range and highly stereoselective D-amino acid dehydrogenase for the one-step synthesis of D-amino acids. *J. Am. Chem. Soc.* **2006,** *128*, 10923-10929.

(27) Dennig, A.; Gandomkar, S.; Cigan, E.; Reiter, T. C.; Haas, T.; Hall, M.; Faber, K. Enantioselective biocatalytic formal α-amination of hexanoic acid to l-norleucine. *Org. Biomol. Chem.* **2018,** *16*, 8030-8033.

(28) Jiang, W.; Fang, B.-S. Construction and evaluation of a novel bifunctional phenylalanine–formate dehydrogenase fusion protein for bienzyme system with cofactor regeneration. *J. Ind. Microbiol. Biotechnol.* **2016,** *43*, 577-584.

(29) Wu, H.; Tian, C.; Song, X.; Liu, C.; Yang, D.; Jiang, Z. Methods for the regeneration of nicotinamide coenzymes. *Green Chem.* **2013,** *15*, 1773-1789.

(30) van der Donk, W. A.; Zhao, H. Recent developments in pyridine nucleotide regeneration. *Curr. Opin. Biotechnol.* **2003,** *14*, 421-426.

(31) Yuan, M.; Sahin, S.; Cai, R.; Abdellaoui, S.; Hickey, D. P.; Minteer, S. D.; Milton, R. D. Creating a low-potential redox polymer for efficient electroenzymatic CO_2 reduction. *Angew. Chem.* **2018,** *130*, 6692-6696.

(32) Cai, R.; Milton, R. D.; Abdellaoui, S.; Park, T.; Patel, J.; Alkotaini, B.; Minteer, S. D. Electroenzymatic C–C bond formation from CO_2. *J. Am. Chem. Soc.* **2018,** *140*, 5041-5044.

(33) Kuk, S. K.; Singh, R. K.; Nam, D. H.; Singh, R.; Lee, J. K.; Park, C. B. Photoelectrochemical reduction of carbon dioxide to methanol through a highly efficient enzyme cascade. *Angew. Chem. Int. Ed.* **2017,** *56*, 3827-3832.

(34) Yuan, M.; Kummer, M.; Milton, R. D.; Quah, T.; Minteer, S. D. Efficient NADH Regeneration by a Redox Polymer-Immobilized Enzymatic System. *ACS Catal.* **2019,** *9*, 5486-5495.

(35) Alkotaini, B.; Abdellaoui, S.; Hasan, K.; Grattieri, M.; Quah, T.; Cai, R.; Yuan, M.; Minteer, S. D. Sustainable Bioelectrosynthesis of the Bioplastic Polyhydroxybutyrate: Overcoming Substrate Requirement for NADH Regeneration. *ACS Sustain. Chem. Eng.* **2018,** *6*, 4909-4915.

(36) Chen, X.; Cao, Y.; Li, F.; Tian, Y.; Song, H. Enzyme-Assisted Microbial Electrosynthesis of Poly (3-hydroxybutyrate) via CO_2 Bioreduction by Engineered *Ralstonia eutropha*. *ACS Catal.* **2018,** *8*, 4429-4437.

(37) Mayr, J. C.; Grosch, J. H.; Hartmann, L.; Rosa, L. F.; Spiess, A. C.; Harnisch, F. Resting *Escherichia coli* as Chassis for Microbial Electrosynthesis: Production of Chiral Alcohols. *ChemSusChem* **2019,** *12*, 1631-1634.

(38) Weckbecker, A.; Gröger, H.; Hummel, W., Regeneration of nicotinamide coenzymes: principles and applications for the synthesis of chiral compounds. In *Biosystems Engineering I*, Springer: Berlin, 2010; pp 195-242.

(39) Milton, R. D.; Cai, R.; Sahin, S.; Abdellaoui, S.; Alkotaini, B.; Leech, D. n.; Minteer, S. D. The in vivo potential-regulated protective protein of nitrogenase in *Azotobacter vinelandii* supports aerobic bioelectrochemical dinitrogen reduction in vitro. *J. Am. Chem. Soc.* **2017,** *139*, 9044-9052.

(40) Plumeré, N.; Rüdiger, O.; Oughli, A. A.; Williams, R.; Vivekananthan, J.; Pöller, S.; Schuhmann, W.; Lubitz, W. A redox hydrogel protects hydrogenase from high-potential deactivation and oxygen damage. *Nat. Chem.* **2014,** *6*, 822.

(41) Lowe, D.; Thorneley, R. The mechanism of *Klebsiella pneumoniae* nitrogenase action. Pre-steady-state kinetics of H_2 formation. *Biochem. J.* **1984,** *224*, 877-886.

(42) Thorneley, R. N.; Lowe, D. The mechanism of *Klebsiella pneumoniae* nitrogenase action. Simulation of the dependences of H_2-evolution rate on component-protein concentration and ratio and sodium dithionite concentration. *Biochem. J.* **1984,** *224*, 903-909.

(43) Koszelewski, D.; Tauber, K.; Faber, K.; Kroutil, W. ω-Transaminases for the synthesis of non-racemic α-chiral primary amines. *Trends Biotechnol.* **2010,** *28*, 324-332.

(44) Wiame, J.; Pierard, A.; Ramos, F., [93] l-Alanine dehydrogenase from *Bacillus subtilis*: L-Alanine+ DPN^++ H_2O⇄ Pyruvate+ $DPNH^+$ + H^++ NH_4^+. In *Methods in Enzymology*, Elsevier: Amsterdam, 1962; pp 673-676.

(45) Schütte, H.; Hummel, W.; Tsai, H.; Kula, M.-R. l-leucine dehydrogenase from *Bacillus cereus*. *Appl. Microbiol. Biotechnol.* **1985,** *22*, 306-317.

(46) Chen, H.; Huang, R.; Kim, E. J.; Zhang, Y. H. P. J. Building a thermostable metabolon for facilitating coenzyme transport and in vitro hydrogen production at elevated temperature. *ChemSusChem* **2018,** *11*, 3120-3130.

(47) Kim, E.-J.; Kim, J.-E.; Zhang, Y.-H. P. J. Ultra-rapid rates of water splitting for biohydrogen gas production through in vitro artificial enzymatic pathways. *Energy Environ. Sci.* **2018,** *11*, 2064-2072.

(48) Chandrayan, S. K.; Wu, C.-H.; McTernan, P. M.; Adams, M. W. High yield purification of a tagged cytoplasmic [NiFe]-hydrogenase and a catalytically-active nickel-free intermediate form. *Protein Expr. Purif.* **2015,** *107*, 90-94.

(49) Badalyan, A.; Yang, Z.-Y.; Seefeldt, L. C. A Voltammetric study of nitrogenase catalysis using electron transfer mediators. *ACS Catal.* **2019,** *9*, 1366-1372.

(50) Xue, Y.-P.; Cao, C.-H.; Zheng, Y.-G. Enzymatic asymmetric synthesis of chiral amino acids. *Chem. Soc. Rev.* **2018,** *47*, 1516-1561.

(51) Li, H.; Zhu, D.; Hyatt, B. A.; Malik, F. M.; Biehl, E. R.; Hua, L. Cloning, protein sequence clarification, and substrate specificity of a leucine dehydrogenase from *Bacillus sphaericus* ATCC4525. *Appl. Biochem. Biotechnol.* **2009,** *158*, 343-351.

(52) Kaufman, S.; Mason, K. Specificity of amino acids as activators and substrates for phenylalanine hydroxylase. *J. Biol. Chem.* **1982,** *257*, 14667-14678.

(53) Qi, Y.; Yang, T.; Zhou, J.; Zheng, J.; Xu, M.; Zhang, X.; Rao, Z.; Yang, S.-T. Development of a multi-enzymatic desymmetrization and its application for the biosynthesis of L-norvaline from dl-norvaline. *Process Biochem.* **2017,** *55*, 104-109.

(54) Hasegawa, S.; Suda, M.; Uematsu, K.; Natsuma, Y.; Hiraga, K.; Jojima, T.; Inui, M.; Yukawa, H. Engineering of *Corynebacterium glutamicum* for high-yield L-valine production under oxygen

deprivation conditions. *Appl. Environ. Microbiol.* **2013,** *79*, 1250-1257.

(55) Parker, W. L.; Hanson, R. L.; Goldberg, S. L.; Tully, T. P.; Goswami, A. Preparation of (S)-1-cyclopropyl-2-methoxyethanamine by a chemoenzymatic route using leucine dehydrogenase. *Org. Process Res. Dev.* **2012,** *16*, 464-469.

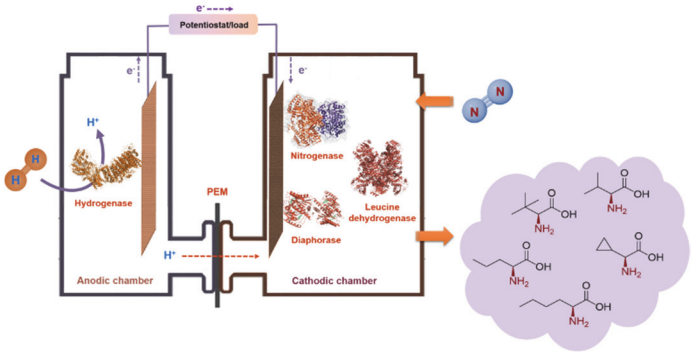
e⁻
Potentiostat/load
e⁻
e⁻
H⁺
H
H
Hydrogenase
PEM
Nitrogenase
Leucine
dehydrogenase
Diaphorase
H⁺
Anodic chamber
Cathodic chamber
N
N
O
OH
NH2